Available online at www.eccomasproceedia.org
Eccomas Proceedia SMART (2023) 619-630

ECCOMAS
Proceedia

X ECCOMAS Thematic Conference on Smart Structures and Materials
SMART 2023
D.A. Saravanos, A. Benjeddou, N. Chrysochoidis and T. Theodosiou (Eds)

ACTIVE LAYERED COMPOSITES: A VARIABLE KINEMATICS APPROACH WITH STIMULUS EXPANSION MODEL

Adrian Ehrenhofer[1,2,*], **Michele D'Ottavio**[3,*], **Olivier Polit**[3], **Thomas Wallmersperger**[1,2]

[1]Institute of Solid Mechanics, Technische Universität Dresden
George-Bähr-Str. 3c, 01062 Dresden

[2]Dresden Center for Intelligent Materials
George-Bähr-Str. 3c, 01062 Dresden

[3]LEME EA4416, Université Paris Nanterre
50, rue de Sèvres 92410 Ville d'Avray

[*] Corresponding authors: Adrian.Ehrenhofer@tu-dresden.de & mdottavi@parisnanterre.fr

Abstract. Active/smart materials are often applied in the form of plate-like composite structures. Therein, they are combined with other (active or passive) materials that serve different purposes, such as providing mechanical counterpoints, protection against multi-field influences, or electrical functionality. Additionally included active materials can also be applied for their sensorics behavior. For an enhanced description of the mechanical response of these plate-like Soft-Hard Active-Passive Embedded Structures (SHAPES), we combine (i) a variable kinematics approach referred to as Sublaminate Generalized Unified Formulation (sGUF) with (ii) the Stimulus-Expansion-Model (SEM) for the description of the active behavior. In the current work, results for SHAPES with polymer gel layers and piezoceramic layers are presented. The current work opens up various possibilities to combine different materials with passive, active, and sensoric capabilities inside a plate-like composite. The promising results call for the implementation of this modeling approach into refined numerical solution models, such as Finite Element or Ritz methods.

Key words: Smart materials, Stimulus Expansion Model, Variable kinematics approach, Piezo-Actuators, Hydrogels, Dielectric Elastomer Actuators

1 INTRODUCTION: Active-passive laminates made from soft and hard layers

Efficient structural models for smart structures allow to assess and optimise their performance, depending on the various design parameters that typically enter the definition of such complex structures. Beyond the conventional parameters related to the macroscale response (dictated by geometry and boundary conditions), also meso- and microscale parameters are of paramount importance. These can be, e.g., the stacking sequence of the active and passive

Peer-review under responsibility of the organizing committee of SMART 2023.
doi: 10.7712/150123.9816.444848

layers, stiffness mismatches, spatially distributed activation stimuli, or the chemo-physical constitution of the smart material. Classical macro-scale models available in commercial computational software are inadequate for accounting for such lower scale effects. On the other hand, the solution of the full continuum mechanics equations – including the thermo-chemo-physical coupling that is typical of smart materials – makes an efficient exploration of the design space clearly impossible.

Soft-Hard Active-Passive Embedded Structures (SHAPES) are composites comprising layers with different stiffness and activity [1, 2]. Their behavior heavily depends on the environment that they are embedded in, because this environment provides the stimulus for their activation/actuation [3]. Different classes of active materials can be used in SHAPES: For example, hydrogels can be designed to respond to multiple stimuli of the environment to form sensors or actuators [4]. They can respond to single or multiple stimuli and their behavior can be represented in a normalized way, to allow the prediction of their swelling behavior [5, 6].

In the current work, we propose a variable kinematics approach for the definition of structural models (beams, plates, shells) of SHAPES. The active behavior is included with a physics-based regression method called Stimulus-Expansion-Model (SEM), allowing to define homogenized properties of the smart material in every layer. The variable kinematics approach provides a virtually infinite number of structural models, ranging from the well known and simple Classical Laminate Theory (CLT) and First-order Shear Deformation Theory (FSDT), up to quasi-3D models, including Equivalent Single Layer (ESL) as well as Layer-Wise (LW) models [7, 8]. This way, it is possible to adapt the computational cost of the structural model depending on the problem at hand and on the output quantity of interest, e.g., a global displacement or a local stress.

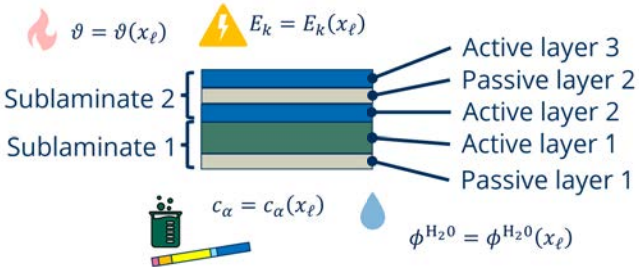

Figure 1: Laminate with different active and passive layers.

The current work is structured as follows: In the following section 2, the Stimulus-Expansion-Model (SEM) and the sublaminate Generalized Unified Formulation (sGUF) are explained. In the results section 3, different active-passive composites are calculated with our combined sGUF-SEM model. The results are compared to literature results and Finite-Element simulations. The conclusion and outlook is given in section 4.

2 METHODS: Modeling of single and multiple active and passive layers

In the current section, the Stimulus-Expansion-Model is explained in section 2.1. This is followed by a description of the sGUF theory in section 2.2. The derivation of the Navier-type solution is shown in section 2.3. Based on this, the results in section 3 are derived.

2.1 Stimulus-Expansion-Model for the inclusion of active behavior

The Stimulus-Expansion-Model allows the inclusion of active behavior by using the analogy between active expansion and thermal expansion [6, 9]. In the current work, the linearized form of the SEM is applied, which we previously used for active hydrogels [10] and Dielectric Elastomer Actuators [11]. The parts of the model for the *static*[1] case are the following:

$$\text{Mechanical balance laws} \qquad \sigma_{kl,k} + f_l = 0, \qquad \sigma_{kl} = \sigma_{lk} \tag{1}$$

$$\text{Stimulus field balance law} \qquad \Psi_{,ii} = \psi \tag{2}$$

$$\text{Kinematics} \qquad \varepsilon_{kl} = \tfrac{1}{2}\left(u_{k,l} + u_{l,k}\right) \tag{3}$$

$$\text{Material law} \qquad \sigma_{kl} = C_{klmn}\left(\varepsilon^{\mathrm{S}}_{mn} - \varepsilon^{\text{active}}_{mn}\right) = C_{klmn}\left(\varepsilon^{\mathrm{S}}_{mn} - \alpha_{mn}\Delta S\right) \tag{4}$$

Here, $\boldsymbol{\sigma}$ denotes the stress, $\boldsymbol{f}$ the external body forces, $\boldsymbol{\varepsilon}$ the linear technical strain, $\boldsymbol{u}$ the displacement, $\boldsymbol{C}$ the elasticity tensor, $\boldsymbol{\alpha}^{\mathrm{S}}$ the stimulus expansion coefficient, and $\Delta S = S - S^{\text{ref}}$ the change in stimulus to a reference stimulus S^{ref}. The stimulus itself can be field resolved, i.e., its distribution is governed by a balance law Equation (2) for a field variable Ψ with a possible source term ψ. Depending on the physics of the described active materials, the stimulus can be, e.g., a derivative of Ψ. For example, Ψ can be the electrostatic potential and the stimulus can be the electric field.

Please note that Einstein's summation convention holds. For $\alpha_{mn} = \alpha^{\mathrm{S,i}}\delta_{mn}$, isotropic expansion with the expansion coefficient $\alpha^{\mathrm{S,i}}$ can be assumed, where $\boldsymbol{\delta}$ denotes the Kronecker-delta. Equation (4) can also be described with the strain expansion coefficients λ_{mn}.

The characteristic of the Stimulus-Expansion-Model is the definition of the active expansion term $\varepsilon^{\text{active}}_{mn}$. This term consists of a stimulus change, denoted as ΔS, and an expansion coefficient, which captures the active behavior. In the current work, different active materials are regarded as layers in an active-passive composite. The physical phenomena lead to active expansion terms as described in the respective below.

As a passive material, polyethylene terepthalate (PET) was chosen. PET is a widely used thermoplastic polymer material from the polyester family. Besides engineering applications, it is also used in liquid containers and clothing. In our previous works, biaxially oriented PET (BOPET), which is a foil material that is drawn in heated form for an increase of in-plane elastic modulus, has been used in combination with hydrogels [10, 12].

The Stimulus-Expansion-Model can be easily applied in Finite Element software tools like Abaqus [1]. However, especially for plate-like laminate setups with a high width-to-height ratio $w/h \gg 1$, multiple elements in each layer are needed to adequately describe the stress and

[1] No inertia influence, time-dependent processes in the stimulus field are equilibrated

strain distributions. This fine meshing leads to a large amount of elements in in-plane direction as well, to avoid degradation of the (3D brick) elements. The proposed implementation into a higher-order plate model thus greatly facilitates the design of plate-like SHAPES. Different kinds of active materials can thus be combined with passive materials, as shown in the following sections.

Piezo-ceramics Piezo-ceramics are crystalline materials that can deform due to electrical potential differences. A typical piezo-material is lead zirconate titanate (PZT) [13, 14]. Depending on the mode in which it is actuated, different effects of the anisotropic behavior are applied. The equations of the electro-mechanically strongly coupled field problem can be written according to the IEEE standard on piezoelectricity [15]. Using the stress-free actuation of the material for a polarization in 3-direction (here: z-direction), the anisotropic expansion coefficients can be derived as

$$\alpha_{xx}^{\mathrm{PZT}} = d_{3\,11}; \quad \alpha_{yy}^{\mathrm{PZT}} = d_{3\,22}; \quad \alpha_{zz}^{\mathrm{PZT}} = d_{3\,33}; \quad \alpha_{ij}^{\mathrm{PZT}} = 0 \;\; \text{for } i \neq j. \tag{5}$$

The stimulus difference is $\Delta S = E_3$, wherein the electric field strength E_3 is obtained by solving the electro-static Poisson's equation of the stimulus field (2) with Ψ being the electrostatic potential and ψ a charge term.

Active Hydrogels Hydrogels are synthethic polymers that swell and deswell in water [4]. A commonly used hydrogel is the temperature-sensitive poly(N-isopropyl-acrylamide) [10]. However, many other polymers with different sensitivities are possible [6, 5]. The isotropic expansion coefficient for hydrogel swelling α^{HG} is derived from free swelling experiments as

$$\alpha_{mn}^{\mathrm{HG}} = \delta_{mn} \frac{\varepsilon^{\vartheta_{\mathrm{ref}}}}{\vartheta - \vartheta_{\mathrm{ref}}}; \qquad \Delta S^{\mathrm{HG}} = \vartheta - \vartheta_{\mathrm{ref}}, \tag{6}$$

where $\varepsilon^{\vartheta_{\mathrm{ref}}}(\vartheta) = (d(\vartheta) - d_{\mathrm{ref}})/d_{\mathrm{ref}}$ is defined through the technical strain in relation to a reference state with reference diameter d_{ref} and reference temperature ϑ_{ref}. By applying the normalization concept from our previous works [6, 16], other hydrogel sensitivities can be included in the Stimulus-Expansion-Model.

The stimulus distribution can be derived by solving the stimulus field equation (2) with Ψ being the temperature and $\psi = 0$. This is the stationary form of Fourier's heat transfer equation without heat sources/sinks, as shown in our previous works [17, 18]. For chemical stimuli, it is Fick's law of diffusion; sources and sinks are chemical reactions there.

Dielectric Elastomer Actuators Dielectric Elastomer Actuators (DEAs) are membranes with dielectric material (e.g. polymers), sandwiched between two flexible electrodes [19, 20, 21]. An increase in voltage leads to the attraction of the electrodes and ensuing Maxwell-stress, which in turn leads to an expansion in the in-plane direction. The expansion coefficients for actuation of DEAs are derived from physics [11]. Volume constancy is assumed and the equation of

Maxwell stress in height-direction is used to derive the active strain (or: actuation strain). The membrane is usually pre-stretched to avoid buckling of the layer under actuation.

The stimulus is the voltage between the electrodes. Due to the homogenized view of the DEA of three layers (electrodes and dielectric medium), the electric field is not resolved in height-direction and equation (2) is not utilized. Instead, the attraction force from Coulomb's law directly leads to a deformation of the 3-layer sandwich structure, which can be implemented as an analog expansion [11].

2.2 Variable kinematics model in sublaminate Generalized Unified Formulation

Reduced-order structural models (1D beam, 2D plates/shells) are formulated in axiomatic sense upon introducing *a priori* assumptions for the kinematic field across the composite stack. A whole family of models can be encompassed by expressing the kinematic constraints in the compact index notation referred to as Carrera Unified Formulation (CUF) [22]. The present work adopts the formal extension of CUF towards the possibility of regrouping adjacent plies in to *sublaminates*: this allows a physically meaningful definition of the smart composite, in which passive sub-structures are functionally separated from the active components, for which dedicated modeling assumptions can be introduced. A brief description of this Sublaminate Generalized Unified Formulation (sGUF) is given next, for more details reference is made to the original paper [23] and its extension to piezoelectric composites [24].

The constrained kinematic field is introduced in the equilibrium equations stated in weak-form by means of the virtual work principle:

$$\int_{\Omega} \left\{ \int_{h} \delta\epsilon_{ij}\, \sigma_{ij}\, \mathrm{d}z \right\} \mathrm{d}x_1\, \mathrm{d}x_2 = \int_{\Omega_{\pm}} \delta u_i\, \bar{t}_i\, \mathrm{d}x_1\, \mathrm{d}x_2 \tag{7}$$

where δ is the variational operator, ϵ_{ij} is the kinematically compatible virtual strain field, that satisfies equation (3)) as well as the kinematic boundary conditions defined at the lateral boundary $\Gamma_u = \partial\Omega \times h$, and σ_{ij} is the symmetric stress tensor defined by the material constitutive law, which may include an active deformation expressed by the adopted stimulus-expansion-model (see equation (4)).

Let the plate be composed of $p = 1, 2, \ldots N_p$ homogeneous *physical plies*, each of thickness h_p, stacked along the $x_3 \equiv z$ direction. In sGUF, the stack is represented as an assembly of $k = 1, 2, \ldots N_k$ *numerical layers* or sublaminates, each having a constant thickness h_k composed of N_p^k adjacent physical plies. In each ply of the sublaminate, the plate kinematics is expressed according to the GUF-type compact notation [25]:

$$u_i^{p,k}(x_1, x_2, \zeta) = \sum_{\alpha_{u_i}=0}^{N_{u_i}^k} F_{\alpha_{u_i}}(\zeta)\, \hat{u}_{\alpha_{u_i} i}^{p,k}(x_1, x_2) \tag{8}$$

Each displacement component u_i is thus modeled independently in each sublaminate by means of the "thickness functions" $F_{\alpha_{u_i}}(\zeta)$. It is worth mentioning that models based on a thickness-wise constant transverse displacement u_3 (i.e., $N_{u_3}^k = 0$) require to use modified constitutive

coefficients in order to introduce the plane stress condition. The coordinate ζ is related to the physical coordinate z depending on whether the N_p^k plies of the k^{th} sublaminate are described in Equivalent Single Layer (ESL) or Layer-Wise (LW) sense. In either case, the "thickness functions" $F_\alpha(\zeta)$ are orthogonal Legendre polynomials that allow to use the classical assembly procedure of, e.g., FEM, for constructing the resultant assumption across the whole composite stack upon enforcing the continuity of the displacement field at adjacent plies and sublaminates, see [23, 26] for more details. The stimulus is described always LW and is constant across each active material ply:

$$\overline{\Delta s}^{p,k}(x_1, x_2, z) = \overline{\Delta \hat{s}}^{p,k}(x_1, x_2) \tag{9}$$

Note that the stimulus needs not to be continuous across adjacent active plies or layers. The prescribed stimulus defines along with the corresponding expansion coefficient the virtual work done by the actuation of the smart material plies.

2.3 Navier-type solution

Upon carrying out the integral across the plate thickness, with due account for all through-thickness derivatives, equation (7) yields two-dimensional equilibrium equations for the plate model. These are here solved in strong-form by referring to the Navier-type solution

$$\hat{u}_{\alpha_1 1}(x_1, x_2) = U_{\alpha_1} \cos\tfrac{m\pi x_1}{a} \sin\tfrac{n\pi x_2}{b} \tag{10a}$$
$$\hat{u}_{\alpha_2 2}(x_1, x_2) = V_{\alpha_2} \sin\tfrac{m\pi x_1}{a} \cos\tfrac{n\pi x_2}{b} \tag{10b}$$
$$\hat{u}_{\alpha_3 3}(x_1, x_2) = W_{\alpha_3} \sin\tfrac{m\pi x_1}{a} \sin\tfrac{n\pi x_2}{b} \tag{10c}$$

where m, n are integers defining the number of half-waves. The strong-form solution for the 2D differential equations is only possible under some stringent limitations: the material plies are required to have orthotropy axes aligned with the plate axes x_1, x_2 and the kinematic boundary conditions must correspond to the "simply-support" conditions

$$u_1(x_1, x_2, z) = 0 \qquad \text{at } x_1 = 0, a \tag{11a}$$
$$u_2(x_1, x_2, z) = 0 \qquad \text{at } x_2 = 0, b \tag{11b}$$
$$u_3(x_1, x_2, z) = 0 \qquad \text{at } x_1 = 0, a \text{ and } x_2 = 0, b \tag{11c}$$

The harmonic representation of equation (10) can be used within a Fourier-series development to express solutions for traction loads and stimuli that are distributed in various shapes over the surface Ω.

For each harmonic, the following linear algebraic system is set up

$$\begin{bmatrix} \boldsymbol{K}_{UU} & \boldsymbol{K}_{UV} & \boldsymbol{K}_{UW} \\ \boldsymbol{K}_{UV}^\top & \boldsymbol{K}_{VV} & \boldsymbol{K}_{VW} \\ \boldsymbol{K}_{UW}^\top & \boldsymbol{K}_{VW}^\top & \boldsymbol{K}_{WW} \end{bmatrix} \begin{bmatrix} \boldsymbol{U} \\ \boldsymbol{V} \\ \boldsymbol{W} \end{bmatrix} = \begin{bmatrix} \boldsymbol{F_{US}} \\ \boldsymbol{F_{VS}} \\ \boldsymbol{F_{WS}} \end{bmatrix} + \begin{bmatrix} \boldsymbol{T_U} \\ \boldsymbol{T_V} \\ \boldsymbol{T_W} \end{bmatrix} \tag{12}$$

whose unknowns are the vectors of the generalised displacement variables that define the through-thickness approximations for the whole composite stack. The external work defined by the actuation stimuli is represented by the vectors $\boldsymbol{F_{US}}$, $\boldsymbol{F_{WS}}$ and $\boldsymbol{F_{WS}}$, external tractions are represented by the vectors $\boldsymbol{T}$. The size of the system only depends on the approximation orders used to define the model. For instance, for a plate composed of N_p plies, an ESL model adopting the classical FSDT kinematics will yield a system with only 5 unknown variables, whereas if FSDT is used for each ply independently ($\mathrm{LD}_{1,0}$ model) there will be $2(N_p+1)+1 = 2N_p+3$ variables.

3 RESULTS: Simulation results for selected active-passive composites

The physics of the active materials according to section 2.1 is implemented into the sublaminate Generalized Unified Formulation according to section 2.2. In the current work, we show results for the validation with a Finite-Element-Model of a hydrogel-PET 2-layer composite (see section 3.1) and the comparison to a standard piezo-testcase (see section 3.2).

To allow the comparison between our sGUF-SEM model and FEM results, they are compared in 2D plane-stress state [27]. Then, the reduced stress formulations must be used to avoid the artificial stiffening of the setup (Poisson locking).

3.1 Validation with a Hydrogel-PET composite

A two-layer composite with an active top layer made of the hydrogel pNiPAAm and a passive bottom layer of PET, as used in our previous works, is regarded [1]. The active material is actuated with a very small temperature change of $\Delta S = 0.1\,\mathrm{K}$ to preserve small deformations. The reference temperature is $T_{\mathrm{ref}} = 32\,^{\circ}\mathrm{C}$.

At the temperature of $31.9\,^{\circ}\mathrm{C}$, the elastic modulus of $E^{\mathrm{HG}} = 0.0014\,\mathrm{MPa}$ and the isotropic expansion coefficient $\alpha^{\mathrm{HG}} = -7.5316\,^{\circ}\mathrm{C}^{-1}$ follow, which leads to an isotropic active strain of $\varepsilon^{\mathrm{active}} = 0.0235$ for the top layer. For the passive bottom layer of PET, the elastic modulus is constant with $E^{\mathrm{PET}} = 2.1\,\mathrm{MPa}$.

For the Abaqus simulation, a total of 3000 quadratic quadrilateral elements of type CPE8H were used in a linear pertubation step. The plane strain state in the cross-section was used. In Figure 2 the displacement and stress distributions for the finite element case and for our combined sGUF-SEM are shown.

An excellent agreement for the in-plane displacement u_x and for the stress σ_{xx} can be found. In u_z, a small discrepancy of 2.5% can be found. From the results, it can be seen that our sGUF-SEM model can adequately predict these distributions for the current two-layer case.

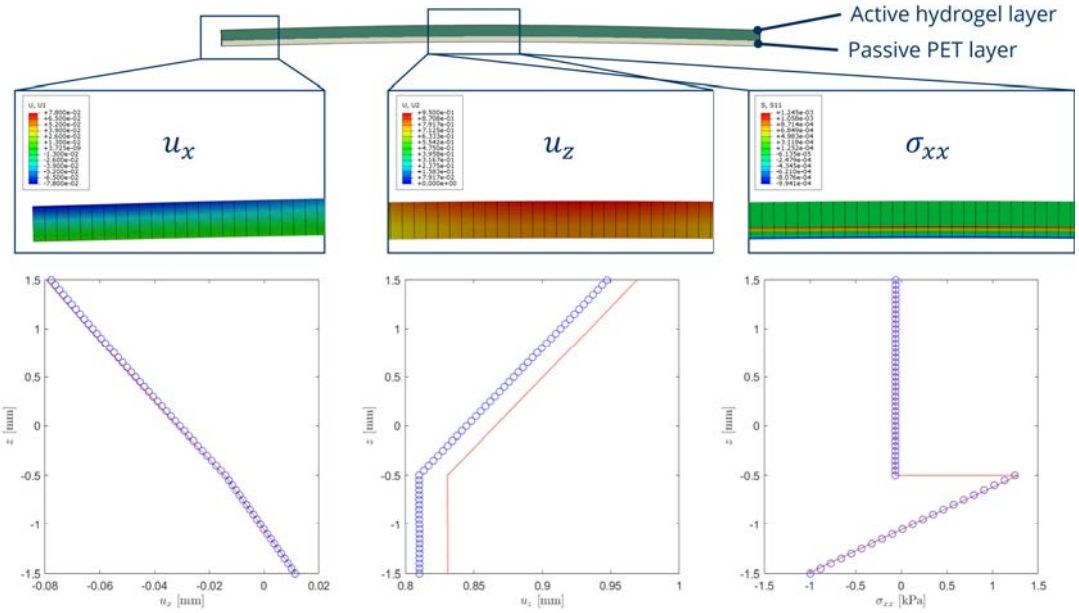

Figure 2: A top active hydrogel layer of $2\,\mathrm{mm}$ height is combined with a bottom passive PET layer of $1\,\mathrm{mm}$ height. The beam length is $100\,\mathrm{mm}$. Bearings are according to the Navier testcase. The distributions of u_x, u_z and σ_{xx} are shown for our current model (solid line) and the finite element results in Abaqus (dots).

3.2 PZT bimorph

A simply-supported two-plies PZT bimorph with parallel polarization is considered in cylindrical bending. The electric actuation is defined by a voltage difference $\Delta V = 50\,\mathrm{V}$ acting uniformly over the total length $L = 25\,\mathrm{mm}$ of the plate and across the thickness of each PZT ply of thickness $h_{\mathrm{PZT}} = \frac{H}{2}$. Different ratios L/H are investigated. Reference solutions and material properties are given in [27, 28]. The solution is obtained as a Fourier series development, in which the stimulus is defined for each harmonic m as

$$\Delta S_m = \frac{\Delta V_m}{h_{\mathrm{PZT}}} = \frac{1}{h_{\mathrm{PZT}}} \frac{4V_0}{m\pi} \tag{13}$$

where $V_0 = 50$ is the potential value prescribed at the outer electrodes, the mid-electrode being grounded $(V = 0)$. Results for $L/H = 10$ are illustrated in Figure 3, where present results are compared against a 3D FEM solution [29].

An excellent agreement is obvious for the in-plane displacement u_x and the bending stress σ_{xx}, while a closer look is required to understand the discrepancies in the out-of-plane deflection u_z. In fact, present results overestimate this deflection by about 5%. The reason is attributed to the constant driving electric field assumed in the present stimulus-expansion model, that disregards the change in electric field due to the bending response, i.e. the induced field produced by the mechanical deformation is not accounted for. To illustrate this, two additional curves are plotted in Figure 3 (b), which are obtained by two variable kinematics CUF-based models LD4 implemented with the full piezoelectric coupling [14]: one model assumes a quadratic electric

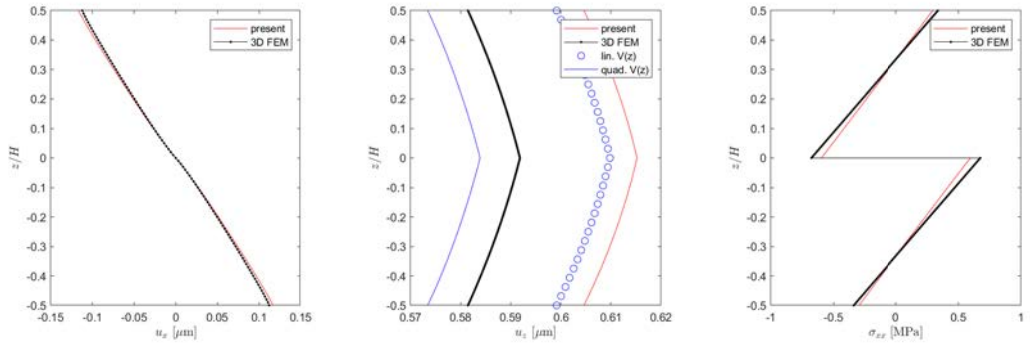

Figure 3: PZT bimorph: validation of the present modeling approach.

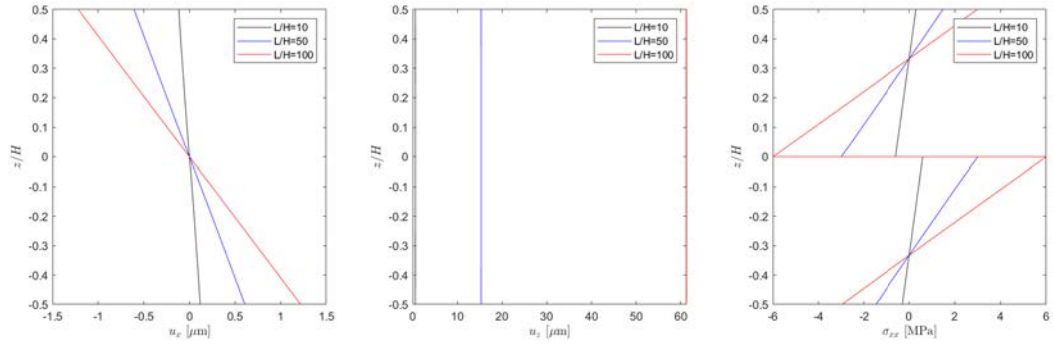

Figure 4: PZT bimorph actuated by $\Delta V = 50\,\mathrm{V}$: influence of the length-to-thickness ratio on the actuation.

potential $V(z)$ across the thickness, and it thus retains the induced electric field produced by the mechanical bending; the other model has only a linear distribution of $V(z)$, which thus neglects the bending-induced field. Comparing these curves it is apparent that the induced field reduces the effective driving field, thus yielding a lower bending deflection.

The influence of the plate thickness on the bimorph actuation is assessed next. The moderately thick $L/H = 10$ bimorph is compared against a thin and a very thin bimorph, with $L/H = 50$ and $L/H = 100$, respectively. The driving voltage difference is kept fixed to $\Delta V = 50\,\mathrm{V}$, which corresponds for the very thin actuator to an electric field intensity of $400\,\mathrm{V/mm}$. Results for the bending deflection and stresses are reported in Figure 4, which show the enhanced actuation capabilities of the thin bimorph.

4 CONCLUSIONS

In the current work, we have shown how the Stimulus-Expansion-Model can be used to implement different active materials into the sublaminate Generalized Unified Formulation description of plates. From the physics of the active materials, expansion coefficients and equivalent stimuli are derived, which are used within the framework of the Stimulus-Expansion-Model. The analytical solutions gained for the Navier solution allow cost-effective parameter variation in comparison to finite element simulations with solid elements. The resulting model can be used for high-throughput calculations for different active-passive and active-active material pairings. This will allow the identification of novel smart composites.

References

[1] A. Ehrenhofer, "Design of soft and hard active-passive composite beams," *Mechanics of Advanced Materials and Structures*, vol. 30, no. 5, pp. 945–960, 2023.

[2] A. Ehrenhofer, "Stiffness pairing in soft-hard active-passive actuators," in *Proceedings in Applied Mathematics and Mechanics*, 2022.

[3] A. Ehrenhofer, M. Elstner, A. Filippatos, M. Gude, and T. Wallmersperger, "Window-opener as an example for environment measurement and combined actuation of smart hydrogels," in *Proc. SPIE 11587, Electroactive Polymer Actuators and Devices (EAPAD) XXIII*, 2021.

[4] G. Gerlach and K.-F. Arndt, *Hydrogel Sensors and Actuators: Engineering and Technology*. Springer Science & Business Media, Berlin Heidelberg, 2009, vol. 6.

[5] A. Ehrenhofer, S. Binder, G. Gerlach, and T. Wallmersperger, "Multisensitive swelling of hydrogels for sensor and actuator design," *Advanced Engineering Materials*, vol. 22, no. 7, p. 2000004, 2020.

[6] A. Ehrenhofer, M. Elstner, and T. Wallmersperger, "Normalization of hydrogel swelling behavior for sensoric and actuatoric applications," *Sensors and Actuators B: Chemical*, vol. 255, no. 2, pp. 1343 – 1353, 2018.

[7] E. Carrera, S. Brischetto, and P. Nali, *Plates and shells for smart structures. Classical and advanced theories for modeling and analysis*. John Wiley & Sons, Ltd, 2011.

[8] E. Carrera, "Theories and finite elements for multilayered plates and shells: a unified compact formulation with numerical assessment and benchmarking," *Archives of Computational Methods in Engineering*, vol. 10, no. 3, pp. 215–296, 2003.

[9] A. Ehrenhofer, M. Hahn, M. Hofmann, and T. Wallmersperger, "Mechanical behavior and pore integration density optimization of switchable hydrogel composite membranes," *Journal of Intelligent Material Systems and Structures*, vol. 31(3), pp. 425–435, 2020.

[10] A. Ehrenhofer, G. Bingel, G. Paschew, M. Tietze, R. Schröder, A. Richter, and T. Wallmersperger, "Permeation Control in Hydrogel-Layered Patterned PET Membranes with Defined Switchable Pore Geometry - Experiments and Numerical Simulation," *Sensors and Actuators B: Chemical*, vol. 232, pp. 499–505, 2016.

[11] M. Franke, A. Ehrenhofer, S. Lahiri, E.-F. M. Henke, T. Wallmersperger, and A. Richter, "Dielectric elastomer actuator driven soft robotic structures with bioinspired skeletal and muscular reinforcement," *Frontiers in Robotics and AI*, vol. 7, p. 178, 2020.

[12] A. Ehrenhofer, T. Wallmersperger, and A. Richter, "Simulation of controllable permeation in PNIPAAm coated membranes," in *Proc. SPIE 9800, Behavior and Mechanics of Multifunctional Materials and Composites 2016*, vol. 980016, 2016, pp. 1–13.

[13] H. Jaffe, "Piezoelectric ceramics," *Journal of the American Ceramic Society*, vol. 41, no. 11, pp. 494–498, 1958.

[14] D. Ballhause, M. D'Ottavio, B. Kröplin, and E. Carrera, "A unified formulation to assess multilayered theories for piezoelectric plates," *Computers & Structures*, vol. 83, no. 15-16, pp. 1217–1235, 2005.

[15] "IEEE Standard on Piezoelectricity," *ANSI/IEEE Std 176-1987*, pp. –, 1988.

[16] A. Ehrenhofer and T. Wallmersperger, "A normalization concept for smart material actuation by the example of hydrogels," *PAMM*, vol. 18, no. 1, p. e201800176, 2018.

[17] D. Mählich, A. Ehrenhofer, and T. Wallmersperger, "Extension of the stimulus expansion model for photo-thermo-sensitive hydrogels," in *Proceedings in Applied Mathematics and Mechanics*, 2022.

[18] D. Mählich, A. Ehrenhofer, and T. Wallmersperger, "Modeling of photo-thermo-sensitive hydrogels by applying the temperature expansion analogy," *Accepted in the Journal of Intelligent Material Systems and Structures*, 2023.

[19] I. A. Anderson, T. A. Gisby, T. G. McKay, B. M. O'Brien, and E. P. Calius, "Multi-functional dielectric elastomer artificial muscles for soft and smart machines," *Journal of Applied Physics*, vol. 112, no. 4, p. 041101, 2012.

[20] C. Keplinger, J.-Y. Sun, C. C. Foo, P. Rothemund, G. M. Whitesides, and Z. Suo, "Stretchable, transparent, ionic conductors," *Science*, vol. 341, no. 6149, pp. 984–987, 2013.

[21] E.-F. M. Henke, S. Schlatter, and I. A. Anderson, "Soft dielectric elastomer oscillators driving bioinspired robots," *Soft robotics*, vol. 4, no. 4, pp. 353–366, 2017.

[22] E. Carrera, M. Cinefra, M. Petrolo, and E. Zappino, *Finite Element Analysis of Structures through Unified Formulation*. Chichester, UK: John Wiley & Sons, Ltd, 2014.

[23] M. D'Ottavio, "A sublaminate generalized unified formulation for the analysis of composite structures," *Composite Structures*, vol. 142, pp. 187–199, 2016.

[24] M. D'Ottavio, L. Dozio, R. Vescovini, and O. Polit, "The Ritz – Sublaminate Generalized Unified Formulation approach for piezoelectric composite plates," *International Journal of Smart and Nano Materials*, vol. 9, no. 1, pp. 1–22, 2018.

[25] L. Demasi, "∞^3 Hierarchy plate theories for thick and thin composite plates: The generalized unified formulation," vol. 84, pp. 256–270, 2008.

[26] M. D'Ottavio, L. Dozio, R. Vescovini, and O. Polit, "Bending analysis of composite laminated and sandwich structures using sublaminate variable-kinematic Ritz models," *Composite Structures*, vol. 155, pp. 45–62, 2016.

[27] A. Fernandes and J. Pouget, "An accurate modelling of piezoelectric multi-layer plates," *European Journal of Mechanics-A/Solids*, vol. 21, no. 4, pp. 629–651, 2002.

[28] A. Fernandes and J. Pouget, "Analytical and numerical approaches to piezoelectric bimorph," *International Journal of Solids and Structures*, vol. 40, no. 17, pp. 4331–4352, 2003.

[29] O. Polit, M. d'Ottavio, and P. Vidal, "High-order plate finite elements for smart structure analysis," *Composite structures*, vol. 151, pp. 81–90, 2016.